

1 **The isotopic record of Northern Hemisphere atmospheric carbon monoxide**
2 **since 1950, implications for the CO budget – Supplementary Material**

3 Z. Wang¹, J. Chappellaz², P. Martinerie², K. Park^{1,*}, V. Petrenko^{3,**}, E. Witrant⁴, T. Blunier⁵, C.
4 A. M. Brenninkmeijer⁶, J. E. Mak¹

5 ¹Institute for Terrestrial and Planetary Atmospheres/School of Marine and Atmospheric
6 Sciences, State University of New York at Stony Brook, Stony Brook, NY 11794, USA

7 ²UJF – Grenoble 1 / CNRS, Laboratoire de Glaciologie et Géophysique de l'Environnement
8 (LGGE) UMR 5183, Grenoble, F-38041, France

9 ³Institute of Arctic and Alpine Research, University of Colorado, Boulder, CO 80309, USA

10 ⁴Grenoble Image Parole Signal Automatique (GIPSA-lab), Université Joseph Fourier/CNRS, BP
11 46, 38 402 Saint Martin d'Hères, France

12 ⁵Centre for Ice and Climate, Niels Bohr Institute, University of Copenhagen, DK-2100
13 Copenhagen, Denmark

14 ⁶Max Planck Institute for Chemistry, PO 3060, 55020 Mainz, Germany

15 * now at: Division of Polar Climate Research, Korea Polar Research Institute, Incheon, South
16 Korea

17 ** now at: Department of Earth and Environmental Sciences, University of Rochester, Rochester,
18 NY, USA

19 Correspondence to: Z. Wang (zhihui.wang@stonybrook.edu)

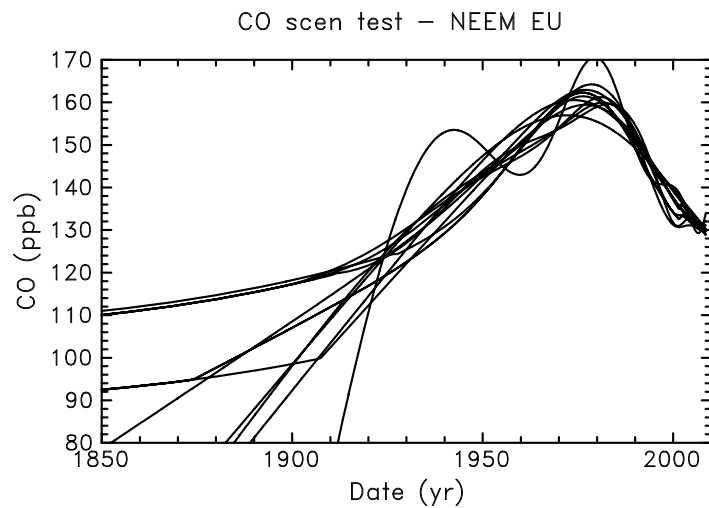
20

21 This document serves as a supplement to ‘The isotopic record of Northern Hemisphere

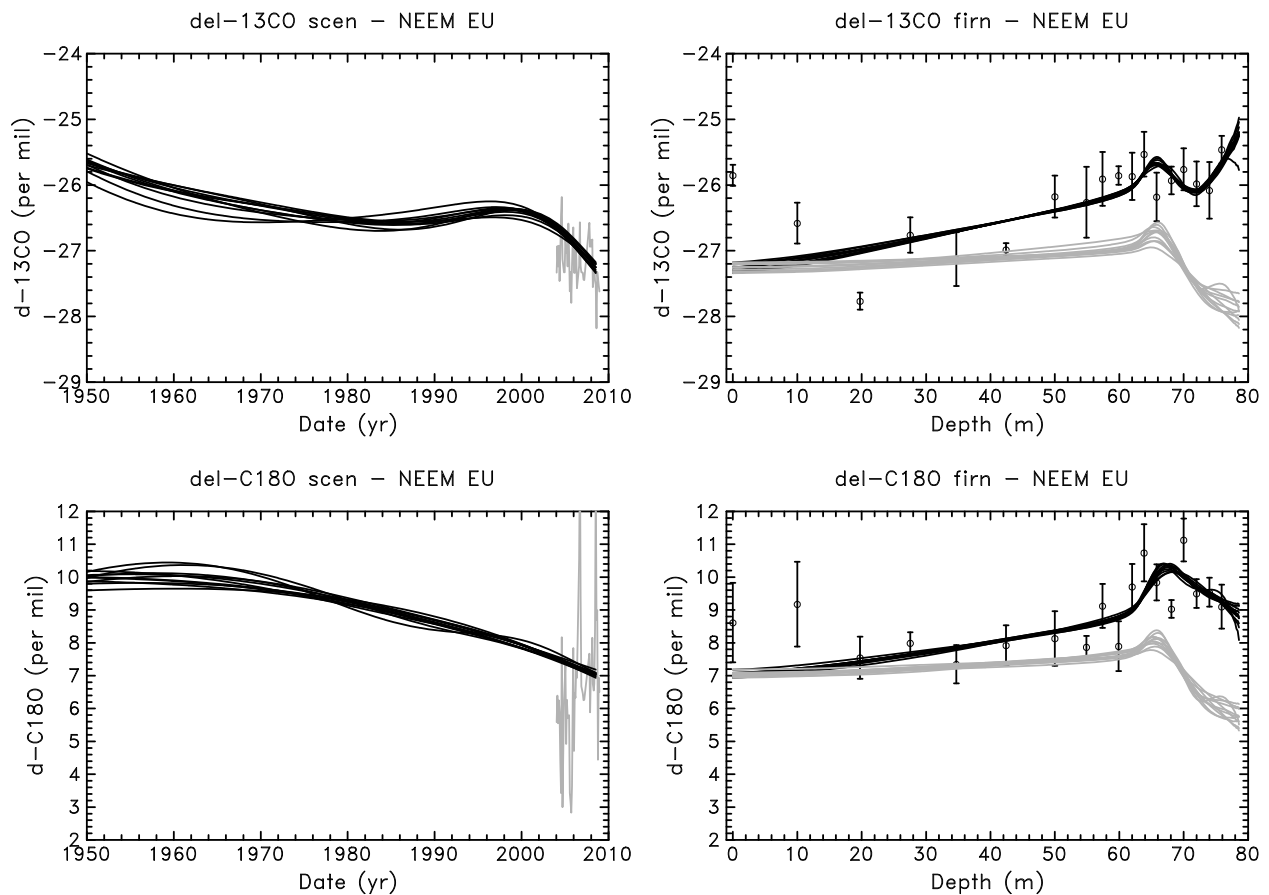
22 atmospheric carbon monoxide since 1950, implications for the CO budget’. It consists of three

23 figures, one table, and some text, which provides additional modeling results that were omitted

24 in the main article in order to improve its readability.



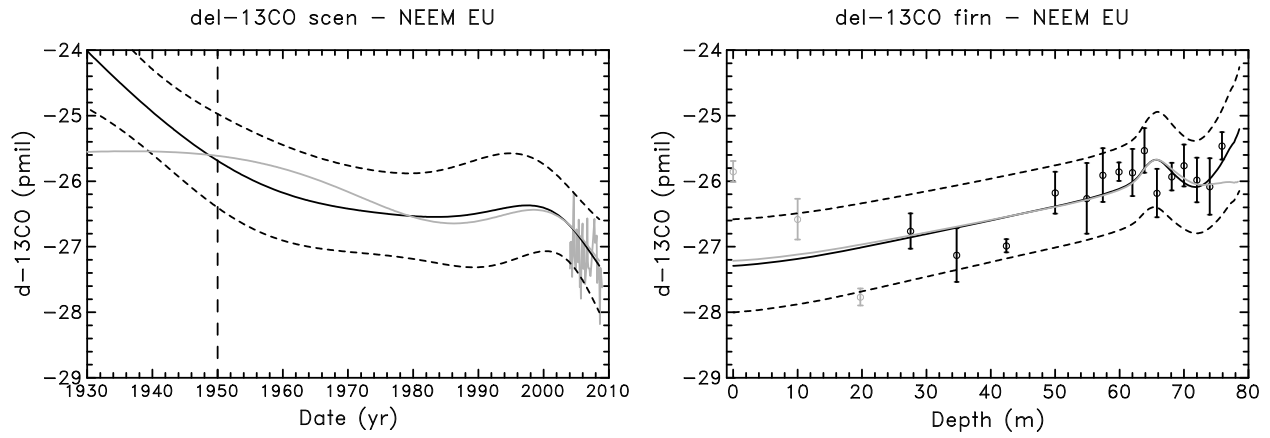
26



27

28 Fig. S1. Estimation of the effect of the CO trend uncertainty on CO isotopes trend
 29 reconstructions. Upper panel: CO scenarios used for the uncertainty test. Medium panel:
 30 reconstructed $\delta^{13}\text{C}$ trends (left) and their matching of firn data in black (right); the grey curves
 31 show the effect of CO trends with a constant atmospheric $\delta^{13}\text{C}$. Lower panel: same as medium
 32 panel for $\delta^{18}\text{O}$.

33



34

35 Fig. S2. Influence of removing the deepest measurement of $\delta^{13}\text{C}$ from the dataset used for
36 atmospheric trend reconstruction. The black lines show the best estimates. The grey lines show
37 the result of a simulation which does not use the deepest $\delta^{13}\text{C}$ measurement as a constraint.
38 Results are shown prior to 1950 in order to visualize the effect of this test on the un-constrained
39 part of the scenario.

40

41

42 Discussion on atmospheric trend of $\delta^{13}\text{C}$

43 Figure S2 shows a $\sim 1.4\text{‰}$ decrease in $\delta^{13}\text{C}$ between 1950 and 2008. Based on the mean values of
44 $[\text{CO}]$ (Fig 4), $[\text{CO}]$ source contributions (Fig 6 and 7) and $\delta^{13}\text{C}$ isotopic signature at Iceland
45 (Emmon et al., in preparation and Table S1), the mass balance calculation can be performed with
46 the following equation:

47
$$\delta^{13}\text{C} = \sum_{i=1}^7 [\text{CO}_i]/[\text{CO}] \times \delta^{13}\text{C}_i \quad (1)$$

48 where $\delta^{13}\text{C}$ is the calculated $\delta^{13}\text{C}$ and i denotes an individual CO source: fossil fuel
49 combustion, methane oxidation, NMHC oxidation, biofuel burning, biomass burning, direct
50 biogenic, and oceanic emission. $[\text{CO}_i]$ stands for CO concentration from each source calculated
51 from $[\text{CO}]$ and the $\delta^{18}\text{O}$ based mass balance model (Fig. 6 and 7) and $[\text{CO}]$ is the atmospheric
52 CO concentration derived from Greenland firn air measurements and diffusion model
53 simulations (Petrenko et al., 2011). $\delta^{13}\text{C}_i$ is the $\delta^{13}\text{C}$ source signature at high northern latitude
54 (Table S1). The results of calculated $\delta^{13}\text{C}$ in 1950-2008 are shown in Fig. S3. We use mean
55 values of $[\text{CO}]$, $\delta^{13}\text{C}$, and $[\text{CO}]$ contribution from each source (Fig 4, 6, and 7) and perform tests
56 related to specific sources of uncertainty. There are two major sources of uncertainties in the
57 $\delta^{13}\text{C}$ mass balance calculation.

58 First the results after 2000 could have large errors due to the method used in the calculation such
59 as the scaling method and the assumptions of constant biofuel emissions in 2005-2008. The
60 biomass burning CO contribution in 2000-2004 is based on the MOZART-4 simulation (Park,
61 2010) and that in 2005-2008 is scaled with the annual biomass burning CO emissions from
62 GFED-v3 (Wiedinmyer et al., 2011), which roughly reflects the real annual biomass burning
63 emissions. The biofuel burning CO contribution in 2000-2004 is based on the MOZART-4

64 simulation (Park, 2010) and that in 2005-2008 is set as the averaged value during 1997 and 2004
65 (Table 1). A possible acceleration of the decrease on calculated $\delta^{13}\text{C}$ occurred after 2000 (Fig.
66 S3). The big jump of $\delta^{13}\text{C}$ in 2002-2003 reflects the big wildfires occurring those years. In the
67 mass balance calculation of the main text, we assign constant annual biomass/biofuel burning
68 CO contribution in 2000-2008, which is 8-year average in 1997-2004 from MOZART-4
69 simulation at Iceland (Table 1) (Park, 2010). For comparison, the calculated $\delta^{13}\text{C}$ based on the
70 assigned constant is also shown in Fig 3S. The decrease in calculated $\delta^{13}\text{C}$ in 2000-2008 by
71 varying annual biomass burning CO contribution is larger than that by fixing annual biomass
72 burning CO contribution.

73 Second, as mentioned in the main text, some of the $\delta^{13}\text{C}$ source signatures are poorly known. The
74 effect of using the estimated maximum and minimum source signatures provided in Table S1 for
75 NMHC oxidation and biomass burning is illustrated by scenarios 1 to 4 on Figure S3. It results in
76 $\delta^{13}\text{C}$ variations by about $\pm 0.5\%$. As source signatures may have changed with time, these
77 uncertainties may also modify the shape of the $\delta^{13}\text{C}$ time trend within the range of results from
78 the four scenarios.

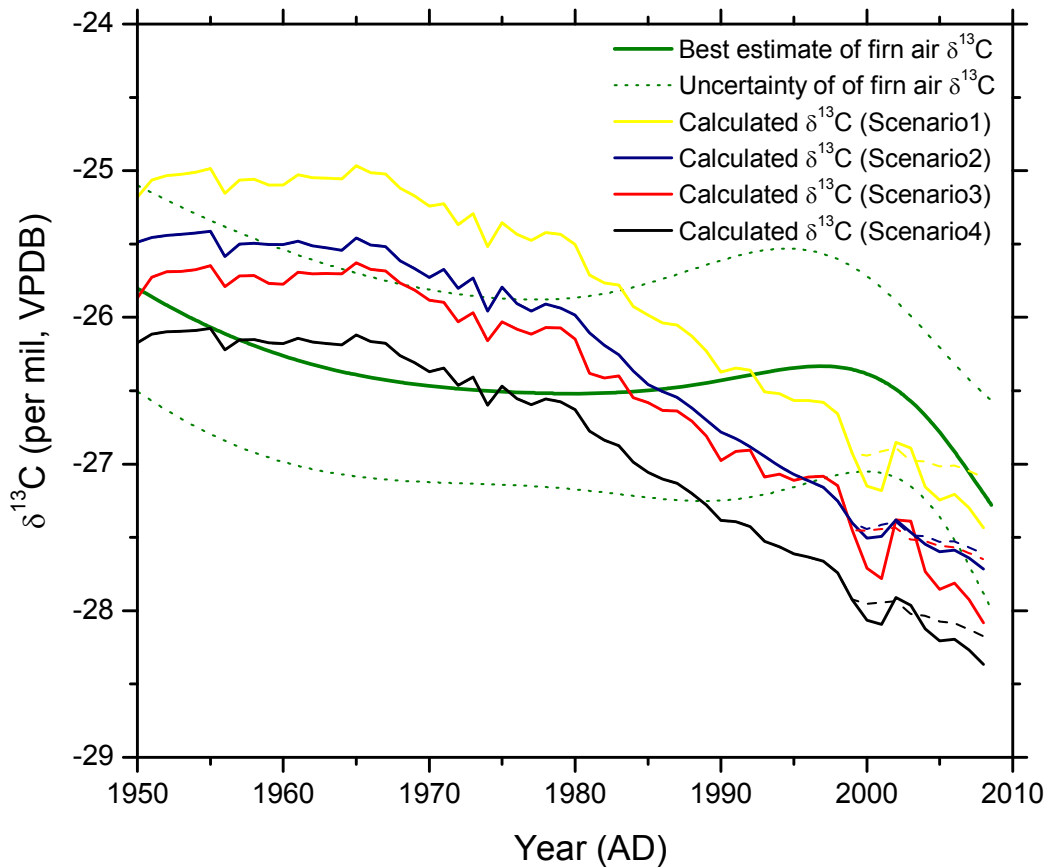
79 We estimate that the increase of methane oxidation (a ^{13}C depleted source) induces a depletion of
80 $\sim 4.2\%$ in the $\delta^{13}\text{C}$ of CO between 1950 and 2008. On the contrary, the fossil fuel combustion
81 results in an enrichment of about 3.9% during the same period. The decrease of $\delta^{13}\text{C}$ caused by
82 all other CO sources except for the above two ranges between 1.3% and 1.6% . Therefore, the
83 decrease of $\delta^{13}\text{C}$ is around $1.6\text{-}1.9\%$ between 1950 and 2008, and the results from this mass
84 balance calculation are consistent with the $\delta^{13}\text{C}$ atmospheric trend inferred from NEEM firn air
85 data within uncertainties on both calculations. Moreover, it has to be pointed out that the small

86 trend in calculated $\delta^{13}\text{C}$ trend is the resultant of compensating effect between larger variations
87 due to individual sources.
88 Overall, the decrease of calculated $\delta^{13}\text{C}$ between 1950 and 2008 is consistent with our derived
89 CO source partitioning and $\delta^{18}\text{O}$ based assumption of a reduced CO production from fossil fuel
90 burning. Our results of CO source partitioning are thus basically validated.
91

92 Table S1. MOZART-4 simulations on atmospheric CO at Iceland in 1997-2004^(a)

Sources	Estimated $\delta^{13}\text{C}$ at Iceland (‰) ^(b)
Fossil fuel	-24
Methane oxidation	-49
NMHC oxidation ^(b)	-18 to -12
Biofuel ^(c)	-21
Biomass burning ^(d)	-11 to -17
Biogenic ^(c)	-26
Ocean	-23

93 ^(a): Data in the table is based on Emmons et al., in preparation and references therein. ^(b): An
 94 arbitrary large range is given to show the possible large uncertainty. ^(c): assume constant C3/C4
 95 ratio in 1950-2008. ^(d): assume C3/C4 ratio is between 3:7 and 7:3 and set it constant in 1950-
 96 2008.



97
98

99 Fig. S3. Comparison of calculated $\delta^{13}\text{C}$ from mass balance calculation and the estimated $\delta^{13}\text{C}$ in
 100 NEEM firm air by LGGE-GIPSA models. Green solid line and dotted lines are the same as those
 101 in Fig. 4. The yellow (Scenario1), blue (Scenario2), red (Scenario3), and black (Scenario4) solid
 102 lines the calculated $\delta^{13}\text{C}$ range based on the different isotopic ratios used (Table S1). Scenario1:
 103 $\delta^{13}\text{C}$ is -11‰ and -12‰ for biomass burning and NMHC oxidation, respectively; Scenario2:
 104 $\delta^{13}\text{C}$ is -17‰ and -12‰ for biomass burning and NMHC oxidation, respectively;
 105 Scenario3: $\delta^{13}\text{C}$ is -11‰ and -18‰ for biomass burning and NMHC oxidation, respectively;
 106 Scenario4: $\delta^{13}\text{C}$ is -17‰ and -18‰ for biomass burning and NMHC oxidation, respectively.
 107 Dashed lines between 2000 and 2008 are results based on an assigned constant annual
 108 biomass/biofuel burning CO contribution, which is 8-year average in 1997-2004 (Park, 2010).

109
110
111
112
113

114 Acknowledgements

115 We sincerely thank Dr. L. Emmons for sharing with us the MOZART-4 simulated CO source
116 contributions data in 2000-2008.

117

118 References

119 Park, K.: Joint Application of Concentration and Isotope Ratios to Investigate the Global
120 Atmospheric Carbon Monoxide Budget: An Inverse Modeling Approach, PhD Thesis, Stony
121 Brook University, USA, 2010.
122 Petrenko, V., Martinerie, P., Novelli, P., Etheridge, D. M., Levin, I., Wang, Z., Petron, G.,
123 Blunier, T., Chappellaz, J., Kaiser, J., Lang, P., Steele, L. P., Vogel, F., Leist, M. A., Mak, J.,
124 Langenfelds, R. L., Schwander, J., Severinghaus, J. P., Forster, G., Sturges, W., Rubino, M., and
125 White, J. W. C.: Records of Northern Hemisphere carbon monoxide and hydrogen back to ~1950
126 from Greenland firn air, Atmospheric Chemistry and Physics, in preparation, 2011.
127 Wiedinmyer, C., Akagi, S. K., Yokelson, R. J., Emmons, L., Al-Saadi, J. A., Orlando, J. J., and
128 Soja, A. J.: The Fire INventory from NCAR (FINN): a high resolution global model to estimate
129 the emissions from open burning, Geoscientific Model Development, 4, 625-641, 2011.
130